UNDERSTANDING AND MANAGING THE SPECTRAL BACKGROUND IN A N_2 ATMOSPHERIC PRESSURE MICROWAVE PLASMA

Richard Morrison, Philip Wilson and Michael Hammer, Agilent Technologies Pty Ltd, 679 Springvale Rd, Mulgrave 3170 Victoria AUSTRALIA

WPC 2012
Poster WP12

Agilent Technologies

Introduction

The 4100 MP-AES is Agilent's newest atomic spectroscopy platform, a microwave plasma (MP) atomic emission spectrometer. It dramatically reduces operating costs by eliminating the need for Ar that is consumed in conventional ICP-OES, and obviates safety hazards by avoiding acetylene and nitrous oxide that are used in AAS. Running on nitrogen, the MP-AES is equally well suited for use in conventional labs and in remote locations. This poster presentation discusses the **plasma speciation, spectroscopy and analytical performance of the instrument** when using nitrogen as the support gas. Detection limits easily surpass those encountered in AAS and for many elements approach those found in ICP-OES.

Fig. 1 The Agilent 4100 MP-AES, microwave plasma atomic emission spectrometer.

Experimental

Emission spectra and analytical measurements were performed on an Agilent 4100 MP-AES. The magnetron is mounted into a waveguide assembly as shown in Fig. 2; details of the microwave cavity are given elsewhere [1]. Fig. 3 shows the optical layout from torch to detector. Emission from the microwave plasma torch is axially viewed and directed by computer-controlled beam steering optics into a Czerny-Turner monochromator, with the dispersed light recorded by a CCD detector. Analyte lines are recorded in fast sequential mode with a spectral resolution of 25-40 pm FWHM, depending on wavelength. Total spectral coverage of the instrument is from 180 nm to 780 nm. Table 1 below lists typical instrument operating parameters and Fig. 4 shows the appearance of the plasma during normal operation.

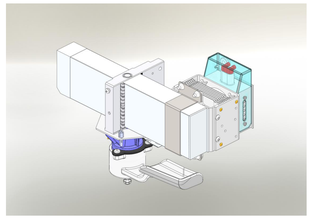

Fig. 2 The magnetron, waveguide, torch loader and torch assembly used in the 4100 MP-AES.

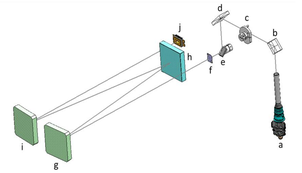

Fig. 3 A schematic diagram of the Agilent 4100 MP-AES : a: torch; b: mirror 1; c: filter assembly; d: mirror 2; e: stepper motor positioned flat-mirror 3; f: entrance slit; g: collimating mirror; h: holographic grating; i: focusing mirror; and j: CCD detector.

Table 1 Agilent 4100 MP-AES technical specifications

Instrument Part	Specifications
Magnetron	2.45 GHz, 400 mA DC,1 kW
Sample Introduction	
Nebulizer	Glass concentric
Spray chamber	Cyclonic
Torch	Modified ICP
Plasma viewing	Axial
Monochromator	
Type	Czerny-Turner
Focal length	600 mm
Collimating mirror	75 mm diameter, spherical
Focusing mirror	87 mm diameter, spherical
Grating	90x90 mm, 2400 lines mm^{-1}
	Blaze wavelength 250 nm
Entrance slit	2.5 mm high x 19 µm wide
Detector	CCD, 532 wide by 128 high, 24x24 µm
	Peltier cooled to 0°C

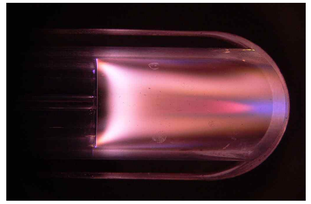

Fig. 4 N_2 MP radial view running 50 ppm Yttrium

Results and Discussion

Plasma Enthalpy and Composition

Fig. 5 shows enthalpy H(T) curves computed using the NASA-CEA Gibbs free energy minimization code [2] for Ar and N_2. Initial slopes reflect different enthalpic contributions for monatomic (T) and diatomic (V,R,T) gases. A rapid increase in N_2 dissociation at elevated temperatures results in a sharp rise in its enthalpy curve. The curve for Ar rises more slowly; upwards curvature is evident when energy is absorbed forming Ar^+. With equivalent input gas flows, enthalpies dictate a lower gas temperature in a N_2 plasma than in Ar.

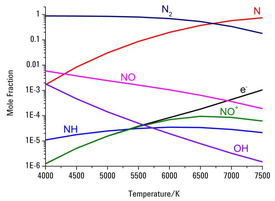

Fig. 6 Simulated N_2 plasma composition introducing aqueous aerosol and water vapour.

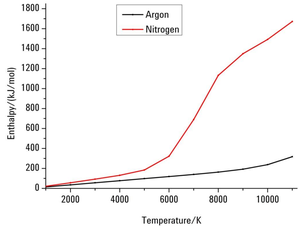

Fig. 5 Enthalpy curves for Ar and N_2 vs temperature and (b) simulation of the N_2 plasma composition with introduction of aqueous aerosol and water vapour (left).

As seen in Fig. 6, the principal charge carriers in a wet N_2 plasma are NO^+ (green) and e^- (black). At T< 6000K we therefore have an **NO plasma** (NO, IE=9.26 eV). The species N_2^*, N_2^{+*}, NO*, NH* and OH* each make contributions to the MP spectral background, as discussed below.

MP Background Emission Spectrum

While the plasma background emission shown in Fig. 7 is complex and highly structured it **is entirely predictable in any region of interest,** as illustrated by the spectrum and simulation shown in Fig. 8. In this region there are spectral contributions from the OH $A(^2\Sigma^+)$-$X(^2\Pi)$ (0,0) band and the N_2 $C(^3\Pi_u)$-$B(^3\Pi_g)$ (1,0) band. The simulation assumes a rotational (gas) temperature of 5000K for both species.

Removal of H_2O (via desolvation) results in spectral contributions from OH, NO and NH being dramatically reduced, resulting in improved detection limits for analyte lines in the 180-340 nm region.

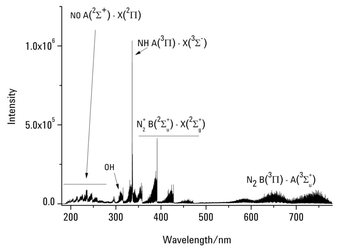

Fig. 7 Full scan N_2 MP emission spectrum of a 1% HNO_3 blank, showing spectral assignments to species/states.

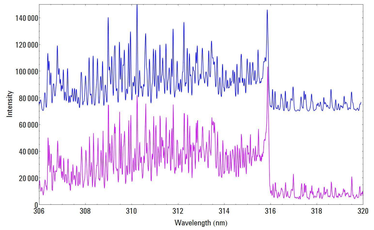

Fig. 8 Expansion of the 306-320 nm MP background. The upper trace (blue) is a computer simulation and the lower trace (purple) is the experimental spectrum.

Results and Discussion

Background Signal Processing

In an Ar plasma (with a smooth background) a simple linear background interpolation between left and right background correction points is usually effective. As seen in Figs. 7 and 8, the structured background in the MP demands a more considered approach.
To achieve near photon noise-limited detection limits, the MP-Expert software employs a spectral modelling technique. Models of the plasma background emission are constructed from replicate readings of blanks, B, blank-subtracted standards S, and interferent species, I. To describe any sample (i.e. unknown) spectrum a linear combination of these models is assumed, with the coefficients b, s and i_j and offset c determined by least squares fitting.

$$U = c + bB + sS + \sum_{j=1}^{n} i_j I$$

Fig. 9 shows a spectrum recorded during measurement of Cu in a high sulfur Zn-Sn-Cu-Pb ore sample (CRM MP-1b) at 223.008 nm. Dashed traces in the vicinity of the analyte peak show the blank term bB and the fit U. Underlying ripples in the spectrum from rotational lines of the NO $A(^2\Sigma^+)$-$X(^2\Pi)$ band system are easily managed by the automatic blank correction option in MPExpert.

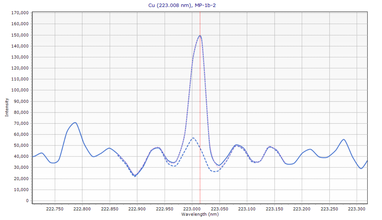

Fig. 9 MP-Expert screen showing the analyte spectrum with the model fit and modelled blank contributions superimposed.

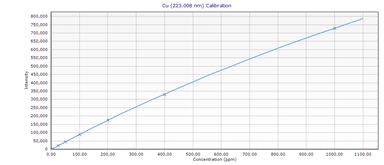

Fig. 10 Calibration curve using the Cu 223.008 nm line to measure a series of Cu standards covering 0-1000 ppm.

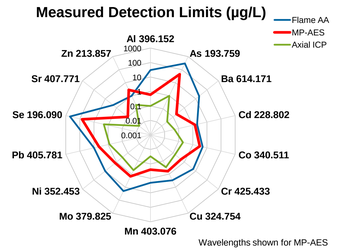

Fig. 11 Detection limit comparison for AAS, MP and ICP-OES.

Detection Limits

The red trace in Fig. 11 shows current detection limits for the MP, plotted on a logarithmic scale. Comparative results using AAS (blue) and axial ICP-OES (green) are also displayed. While the MP's performance is significantly better than AAS it is not generally as good as axial ICP – the N_2 plasma is cooler. The differences between the MP and ICP performance are greatest for analyte lines having higher excitation energies, such as Cd, Zn, As and Se. Work currently underway using desolvation to reduce the spectral background from OH, NO and NH will lead to significant improvements in performance in this regard.

Conclusions

The Agilent 4100 easily outperforms atomic absorption and for many elements approaches the performance of ICP-OES. Although the spectral background is more complex when running with nitrogen, this background is well understood and is managed by the intuitive, easy-to-use MP-Expert software. Very significant paybacks result from the low instrument running costs (by avoiding the need for Ar) and significant safety issues are also addressed by not requiring flammable gases.

References

1. Michael R. Hammer, Spectrochimica Acta Part B 63 (2008) 456-464.
2. http://www.grc.nasa.gov/WWW/CEAWeb/